Effects of Introducing Silicon Isosteres in COX-2 Inhibitors: A Preliminary *In Silico* Evaluation

Patrick Englebienne*

Biocybernetics Unit, Free University of Brussels and Englebienne & Associates, Strijpstraat 21, B-9750 Zingem, Belgium

Abstract: Since the discovery that the anti-inflammatory effects of cyclooxygenase (prostaglandin endoperoxide H_2 synthetase; COX) inhibitors were dependent on their selectivity for the inducible COX-2 isoform over the constitutive COX-1, many efforts have been devoted towards the design of compounds displaying improved COX-2 selectivity. Classical bioisosteres such as CH-CF and CH_2-S/O substitutions have been extensively used in the design of the classical COX-2 inhibitors, although silicon isosteres have been so far overlooked. The replacement of a carbon by a silicon atom can have beneficial effects in this particular family of compounds, because the increased bond lengths and altered bond angles brought by the sila-substitution might modify their binding mode to the COX enzymes. In order to evaluate such possible benefits, several well-characterized model inhibitors were selected and docked in the murine COX-2 and COX-1 binding sites. The binding energies for the interaction of each model compound with the respective isoenzymes were derived from the docking data. As in previous publications, these were found to correlate closely (r^2 = 0.66 and 0.75 for COX-2 and COX-1, respectively) with experimental inhibitory activities towards the recombinant enzymes gathered from the literature. These relationships allowed the prediction of the inhibitors activity towards both enzyme isoforms, which further permitted the prediction of their selectivity for COX-2 with an acceptable accuracy (cross-validated squared correlation coefficient q^2 = 0.64). These model compounds were theoretically modified by substituting selected carbon atoms by an sp^3 silicon, and further docked in both COX-2 and COX-1 binding sites in order to derive their predicted inhibitory activity for both isoforms. Except in a few cases, the sila-substitution did not significantly increase the inhibitory activity towards COX-2. In most cases however, it produced a significant decrease in the inhibitory activity towards COX-1. These results indicate that isosteric sila-substitutions could be of value in the design of COX inhibitors with improved selectivity for COX-2.

Key Words: COX inhibitors, COX-2 selectivity, sila-substitution, silicon bioisostere, *in silico* study, docking, NSAID.

INTRODUCTION

The many physiological roles of prostaglandins (PGs) are now fully recognized. In particular, they exert cytoprotective effects on the gastric mucosa and are critical for normal renal function [1]. Moreover, they trigger inflammation, and the inhibition of their synthesis at inflammatory sites constitutes one of the best approaches to control inflammation [2]. PG H_2 is produced by the catalytic conversion of arachidonic acid by cyclooxygenase (PG endoperoxide H_2 synthetase, COX) isoforms 1 and 2, as a first step in PG synthesis [3]. COX-1 is constitutively expressed and is considered to be responsible for the physiological roles of PGs. In contrast, COX-2 is induced by mitogenic and pro-inflammatory stimuli [4] and induces undesired effects at inflammatory sites, such as pain. Classical, non-steroidal anti-inflammatory drugs (NSAIDs) like aspirin and ibuprofen, non-selectively target both isoforms of the enzyme and consequently, long-term users develop undesirable side effects including gastric membrane degradation and renal failure [5]. Many efforts are therefore spent on the design of selective COX-2 inhibitors as NSAIDs, with significantly reduced side effects. More recently, COX-2 has also been suggested to play a significant role in tumor angiogenesis and selective inhibitors have been proposed as anti-angiogenic agents [6]. Selectivity in COX-2 inhibition by NSAIDs therefore constitutes an increasingly interesting challenge of current drug design.

Like aspirin, many early developed COX inhibitors such as indomethacin and flurbiprofen were found to bind at the active sites of both COX-1 and COX-2 with little specificity. As the overall structure of both COX isoforms is highly conserved, it took some time to identify the significant aspects of an inhibitor structure granting selectivity for COX-2, which was made possible with the subsequent development of the bicyclic nimesulide [7]. During this period, many efforts were spent by pharmaceutical laboratories to model, synthesize and assess the selectivity of several tricyclic compounds for COX-2 inhibition, as it was found that the binding site of the latter isoform was larger than that of COX-1, due to an Ile-Val substitution at residue 523 [7]. The shorter Val in COX-2, makes it indeed possible for compounds to reach an accessory secondary binding pocket, the entrance to which is restricted by the longer Ile side chain of COX-1. Many of these compounds were modeled after the tricyclic 1,5-diarylpyrazole Sc-558 (**1**) (Fig. (**1**)), which had earlier been used, along with the non-selective flurbiprofen, to elucidate the structural bases for selective COX-2 inhibition by X-ray crystallography [8]. The development of this series of compounds led to the

*Address correspondence to this author at the Biomedical Consultant, Englebienne & Associates, Strijpstraat 21, B-9750 Zingem, Belgium; E-mail: penglebienne@pharmadiagnostics.com

1573-4064/05 $50.00+.00

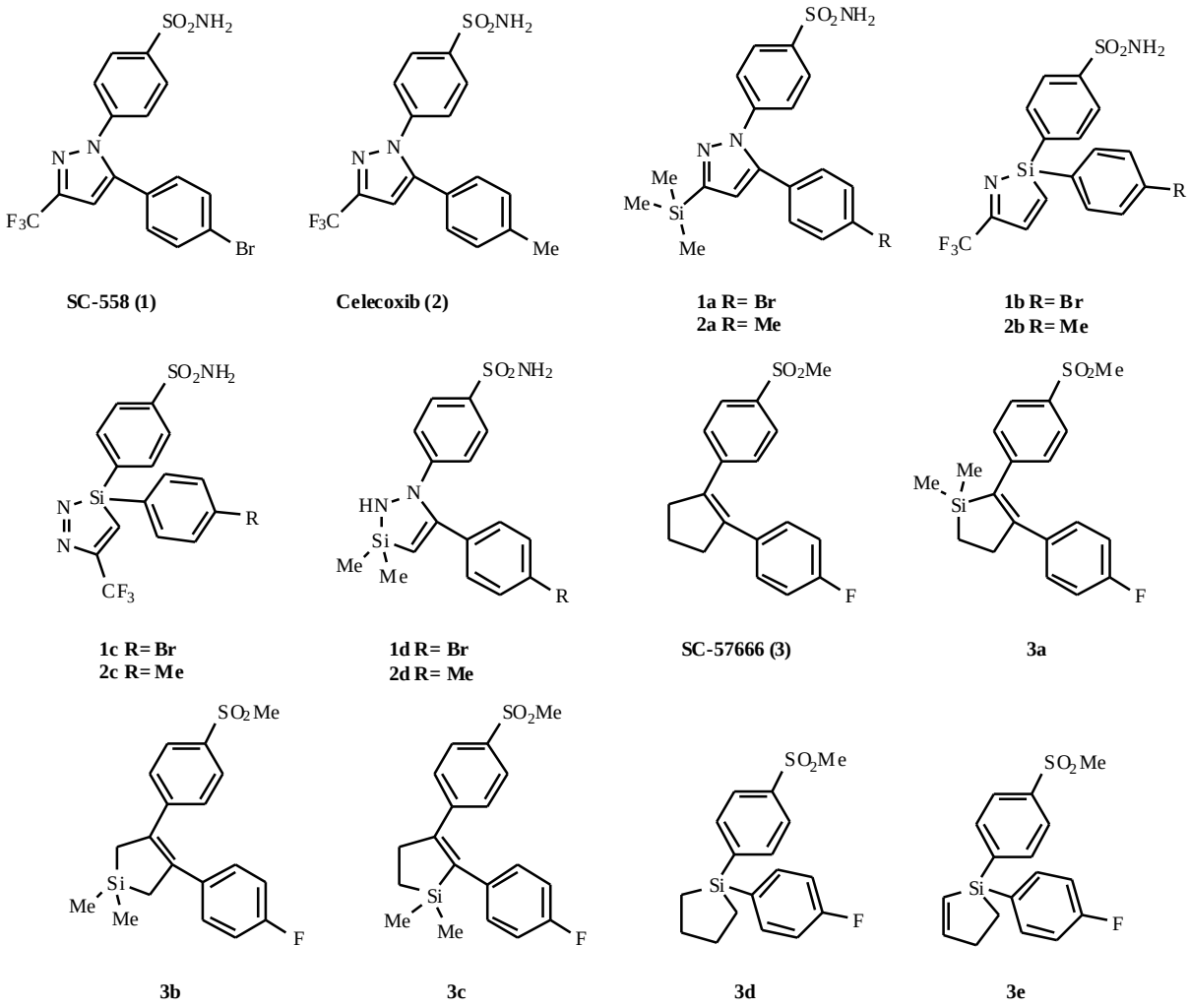

Fig. (1). Structures of the model compounds Sc-558 (**1**), Celecoxib (**2**) and Sc-57666 (**3**) used in the present study and of their sila-substituted derivatives (**1a-d**, **2a-d** and **3a-e**) compared for COX activity and selectivity.

synthesis of the metabolically more labile Celecoxib (**2**) (Fig (**1**)), which is nowadays a model of selective COX-2 inhibitors having reached the market [9]. That early development was based on the further derivatization of the 2,3-diaryl bromothiophene DuP 697, which was one of the original leads beside nimesulide [9]. This progressive and successful development of selective COX-2 inhibitors made ample use of classical bioisosteric replacements from the original lead such as CH/CF and CH_2/S/O, as exemplified by the Sc-558/Celecoxib series (Fig. (**1**)), and the Valdecoxib (**4**), Rofecoxib(**5**) and Etoricoxib (**6**) derivatives (Fig (**2**)) that were subsequently developed [10 - 12]. Further developments also led to the replacement of the sulfonylamide and methanesulfonyl substituents by azido [13], sulfonylazide [14] and methanesulfonamide [15] bioisosteres, respectively, yielding compounds with improved COX-2 selectivity.

An isosteric replacement that remains so far unexplored in COX inhibitors is the carbon/silicon exchange (sila-substitution) [16]. Because the bonds in Si-containing molecules are longer than in the corresponding carbon analogs and the Si-bond angles are altered, the author considered it worth examining the possible improvements in selectivity for COX-2 that could be brought by sila-substitutions at strategic positions in COX inhibitors. Indeed, selectivity is known to be governed by preferential interactions of the inhibitor with selected residues in the binding sites of both COX isoforms [17]. Therefore, a change in length and/or geometry as induced by a sila-substitution was hypothesized to possibly favor or in contrast disfavor, specific interactions within the respective binding sites. In order to gain a preliminary insight into such possibilities, a series of selective COX-2 inhibitor models were imaginatively sila-substituted and computational docking was used to evaluate their interactions within the binding sites of both COX isoforms. Such *in silico* evaluation is indeed recognized to offer speed and an acceptable level of accuracy in small drug discovery programs [18, 19]. The results reported in this study indicate that the isosteric sila-substitution might be of benefit in the design of COX-2 inhibitors with improved selectivity and tissue distribution.

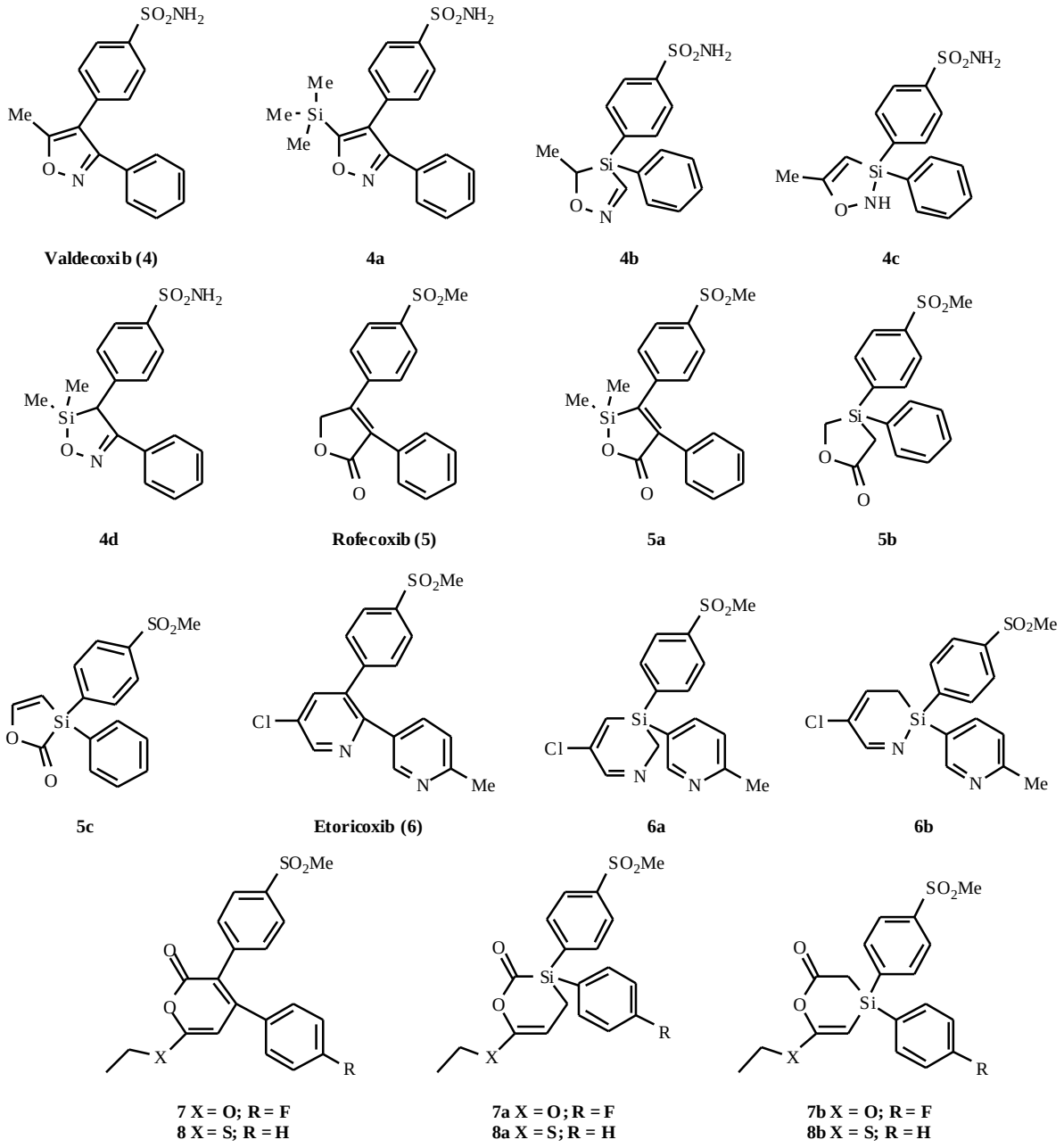

Fig. (2). Structures of the model compounds Valdecoxib (**4**), Rofecoxib (**5**), Etoricoxib (**6**) and two diarylpyran-2-ones (**7** and **8**) used in the present study and of their respective sila-substituted derivatives (**4a-d**, **5a-c**, **6a-b**, **7a-b** and **8a-b**) compared for COX activity and selectivity.

CHEMISTRY

Selective COX-2 inhibitors are tricyclic compounds made of a central 5- or 6-membered cycle C (usually an heterocycle) substituted by two 6-membered rings (A and B) at adjacent positions. Phenyl ring A is further *p*-substituted by a sulfonylamide or a methanesulfonyl group, and B is either a phenyl of an heteroaryl ring left unsubstituted, or *p*-substituted by a methyl group or an halogen atom, respectively. A series of 11 compounds with different C cycles that have been extensively described in the literature were selected for the study (see Figs. (**1**) to (**3**) for the structures). Besides the 1,5-diarylpyrazoles Sc-558 (**1**) and celecoxib (**2**) [9], Sc-57666 (**3**), an earlier 1,2-diarylcyclopentene, was also selected because of its high selectivity for COX-2 [20]. Other model compounds selected, included the 3,4-diarylpyrazole Valdecoxib (**4**), the 3,4-diaryl-2-furanone Rofecoxib (**5**), the 4,5-diaryl-3-furanone (**9**) [21], the 3-phenyl-[2,3']bipyridinyl Etoricoxib (**6**), two 3,4-diarylpyran-2-ones (**7** and **8**) [22], and two 1,2-diarylimidazoles (**10** and **11**) [23]. The model compounds were imaginatively sila-substituted (see Figs (**1**) to (**3**)), whilst keeping in mind the possibilities offered by silicon synthetic chemistry. More

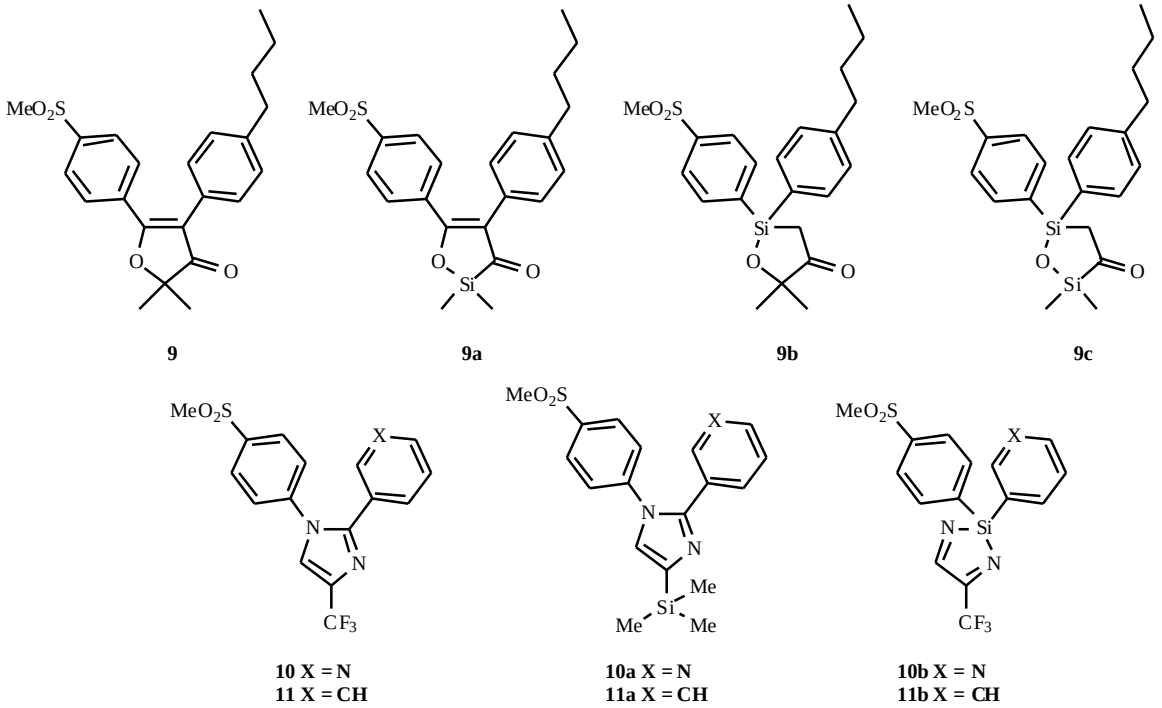

Fig. (3). Structures of the diarylfuran-3-one (**9**), and of the two diarylimidazoles (**10** and **11**) used as model compounds in the present study and of their respective sila-substituted derivatives (**9a-c**, **10a-b** and **11a-b**) compared for COX activity and selectivity.

specifically, three approaches were used. In the first approach (compounds **1a**, **2a**, **4a**, **10a** and **11a**), the C cycle of the model compound was substituted by a trimethylsilanyl group in replacement of either the original methyl, or trifluoromethyl substituent. A silanyl substituent was not considered because it would be cleaved in water to form the corresponding silanol [16]. The regioselective silylation of aromatic C-H bonds has been reported in good yields by several groups, using either ruthenium [24, 25] or nickel [26] derivatives as catalysts. In the second approach (compounds **1d**, **2d**, **3a-c**, **4d**, **5a** and **9a**), an intramolecular substitution was effected in cycle C of a carbon (usually the one substituted by a methyl or trifluoromethyl group in the model compound) by a dimethyl-substituted silicon atom. Finally, in the third approach (compounds **1b**, **1c**, **2b**, **2c**, **3d**, **3e**, **4b**, **4c**, **5b**, **5c**, **6a**, **6b**, **7a**, **7b**, **8a**, **8b**, **9b**, **9c**, **10b**, and **11b**), rings A and B were both attached to a silicon atom replacing either a carbon or a nitrogen atom (**1b**, **2b**) of cycle C, so as to link both rings A and B together at one of their respective original positions in the model compounds. In support to the second and third approaches, let us mention that various synthetic methodologies have been worked out to obtain in good yield, dimethyl or diaryl 1,1-substituted siloles [27, 28] or silaheterocycles [29 - 32]. Such synthetic bioisosteric sila-substitutions in existing drugs have been pioneered in the last decade [16, 33] and are nowadays culminating with such complex structures as those of enantiomeric silicon-containing analogs of piperiden or difenidol, which are subtype-selective muscarinic receptor antagonists [34, 35], of sila-analogs of spiro[indane-1,4'-piperidines], which are selective dopamine and serotonin receptors ligands [36], or of the niguldipine calcium channel and α_1-adrenoreceptor antagonists [37], respectively. The chemical names and physico-chemical characteristics of the compounds considered for this study are listed in Table **1**.

RESULTS AND DISCUSSION

The sila-substitution offers several advantages in drug design, inherent not only to the increased length of the Si-C versus C-C bond, but also to the physical characteristics of silicon [16]. The Si-C bond (1.87 Å) is increased by 20% when compared to the C-C bond (1.54 Å), which induces subtle changes in the size and shape of a molecule. Such changes can be beneficial to the interaction with specific proteins of the silicon analog in comparison to the carbon model counterpart. For instance, in dopamine and serotonin receptor ligands, a sila-substitution increases the affinity from 6- up to 37-fold [36], whilst in muscarinic receptor antagonist it results not only in an increased affinity, but also in an improvement of selectivity towards receptor subtypes [34, 35]. Silicon-containing analogs are also more lipophilic than their carbon counterparts. A small increase in drug lipophilicity results in a marked increase in its volume of distribution, and as a consequence, the drug penetrates more deeply into tissues and is less prone to hepatic metabolism [16]. These potential advantages led to consider the design of the present study intended to evaluate the theoretical application of the sila-substitution to selective COX-2 inhibitors. As expected, the replacement of a carbon by a silicon atom in these molecules (Figs. (**1**) to (**3**)) induced changes in their physico-chemical characteristics (Table **1**). Both volume and surface of the silicon-analog molecules were increased versus their model compounds by 1-2% in

Table 1. Identification and Physico-Chemical Characteristics of the Model and Sila-Substituted Compounds Evaluated

#	Common Name	IUPAC name	M.W.	Molecular Volume (Å^3)	Molecular Surface (Å^2)	Calculated Log P
1	Sc-558	4-[5-(4-Bromophenyl)-3-trifluoromethyl-pyrazol-1-yl]-benzenesulfonamide	446.24	294.14	345.42	3.62
1a		4-[5-(4-Bromophenyl)-3-trimethylsilanyl-pyrazol-1-yl]-benzenesulfonamide	450.43	338.07	400.64	3.94
1b		2-(4-Bromophenyl)-2-(4-methanesulfonylphenyl)-5-trifluoromethyl-2*H*-[1,2]azasilole	461.33	299.88	351.88	3.87
1c		4-[3-(4-Bromophenyl)-5-trifluoromethyl-3*H*-[1,2,3]diazasilol-3-yl]-benzenesulfonamide	462.32	296.3	351.37	3.86
1d		4-[5-(4-Bromophenyl)-3,3-dimethyl-2,3-dihydro-[1,2,3]diazasilol-1-yl]-benzenesulfonamide	424.39	311.34	367.02	3.57
2	Celecoxib	4-(5-*p*-Tolyl-3-trifluoromethyl-pyrazol-1-yl)-bezenesulfonamide	381.37	289.80	345.76	3.27
2a		4-(5-*p*-Tolyl-3-trimethylsilanyl-pyrazol-1-yl)-bezenesulfonamide	385.56	333.58	398.97	3.56
2b		4-(2-*p*-Tolyl-5-trifluoromethyl-2*H*-[1,2]azasilol-2-yl)-bezenesulfonamide	396.46	295.19	350.14	3.47
2c		4-(3-*p*-Tolyl-5-trifluoromethyl-3*H*-[1,2,3]diazasilol-3-yl)-bezenesulfonamide	397.45	292.24	350.55	3.81
2d		4-(3,3-Dimethyl-5-*p*-tolyl-2,3-dihydro-[1,2,3]diazasilol-1-yl)-bezenesulfonamide	359.52	306.9	367.52	3.14
3	Sc-57666	1-(4-Methanesulfonylphenyl)-2-(4-fluorophenyl)-cyclopentene	316.39	272.64	321.73	3.77
3a		4-(4-Fluorophenyl)-5-(4-methanesulfonylphenyl)-1,1-dimethyl-2,3-dihydro-1*H*-silole	360.52	311.13	367.26	4.25
3b		3-(4-Fluorophenyl)-4-(4-methanesulfonylphenyl)-1,1-dimethyl-2,5-dihydro-1*H*-silole	360.52	317.88	386.45	4.29
3c		5-(4-Fluorophenyl)-4-(4-methanesulfonylphenyl)-1,1-dimethyl-2,3-dihydro-1*H*-silole	360.52	312.76	371.21	4.26
3d		1-(4-Fluorophenyl)-1-(4-methanesulfonylphenyl)-silolane	334.48	281.14	331.58	3.83
3e		1-(4-Fluorophenyl)-1-(4-methanesulfonylphenyl)-2,3-dihydro-1*H*-silole	332.47	272.90	322.16	3.83
4	Valdecoxib	4-(5-Methyl-3-phenyl-isoxazol-4-yl)-benzenesulfonamide	314.36	258.3	301.26	3.30
4a		4-(3-Phenyl-5-trimethylsilanyl-isoxazol-4-yl)-benzenesulfonamide	372.52	313.36	364.36	3.78
4b		4-(5-Methyl-4-phenyl-4,5-dihydro-[1,2,4]oxazasilol-4-yl)-benzenesulfonamide	332.45	265.86	307.12	2.36
4c		4-(5-Methyl-3-phenyl-2,3-dihydro-[1,2,3]oxazasilol-3-yl)-benzenesulfonamide	332.45	263.26	312.57	2.94
4d		4-(5,5-Dimethyl-3-phenyl-4,5-dihydro-[1,2,5]oxazasilol-4-yl)-benzenesulfonamide	346.48	293.06	349.78	3.43
5	Rofecoxib	4-(4-Methanesulfonylphenyl)-3-phenyl-5*H*-furan-2-one	314.36	262.18	308.11	2.51

(Table 1. Contd….)

#	Common Name	IUPAC name	M.W.	Molecular Volume (Å^3)	Molecular Surface (Å^2)	Calculated Log P
5a		3-(4-Methanesulfonylphenyl)-2,2-dimethyl-4-phenyl-2*H*-[1,2]oxasilol-5-one	358.49	301.39	352.29	3.44
5b		3-(4-Methanesulfonylphenyl)-3-phenyl-[1,3]oxasilolan-5-one	332.45	270.98	318.25	3.35
5c		3-(4-Methanesulfonylphenyl)-3-phenyl-3*H*-[1,3]oxasilol-2-one	330.43	259.92	304.57	3.03
6	Etoricoxib	5-Chloro-3-(4-methanesulfonylphenyl)-6'-methyl-[2,3']bipyridinyl	358.84	294.24	345.4	2.78
6a		5-Chloro-3-(4-methanesulfonylphenyl)-3-(6-methylpyridin-3-yl)-2,3-dihydro-[1,3]azasiline	376.93	298.36	350.75	3.08
6b		5-Chloro-2-(4-methanesulfonylphenyl)-2-(6-methylpyridin-3-yl)-2,3-dihydro-[1,2]azasiline	376.93	301.91	356.09	3.34
7		6-Ethoxy-4-(4-fluorophenyl)-3-(4-methanesulfonylphenyl)-pyran-2-one	388.41	316.96	369.96	2.24
7a		6-Ethoxy-4-(4-fluorophenyl)-3-(4-methanesulfonylphenyl)-3,4-dihydro-[1,3]oxasilin-2-one	406.50	321.95	371.67	2.83
7b		6-Ethoxy-4-(4-fluorophenyl)-4-(4-methanesulfonylphenyl)-3,4-dihydro-[1,4]oxasilin-2-one	406.50	323.66	381.62	2.82
8		6-Ethylsulfanyl-3-(4-methanesulfonylphenyl)-4-phenyl-pyran-2-one	386.49	322.67	375.62	2.95
8a		6-Ethylsulfanyl-3-(4-methanesulfonylphenyl)-3-phenyl-3,4-dihydro-[1,3]oxasilin-2-one	404.58	327.82	377.99	3.59
8b		6-Ethylsulfanyl-4-(4-methanesulfonylphenyl)-4-phenyl-3,4-dihydro-[1,4]oxasilin-2-one	404.58	330.20	388.04	3.51
9		4-(4-Butylphenyl)-5-(4-methanesulfonylphenyl)-2,2-dimethyl-furan-3-one	398.52	363.33	432.66	3.24
9a		4-(4-Butylphenyl)-5-(4-methanesulfonylphenyl)-2,2-dimethyl-[1,2]oxazasilol-3-one	414.59	369.08	439.82	3.93
9b		4-(4-Butylphenyl)-2-(4-methanesulfonylphenyl)-5,5-dimethyl-[1,2]oxasilolan-4-one	416.61	372.22	444.28	3.56
9c		5-(4-Butylphenyl)-5-(4-methanesulfonylphenyl)-2,2-dimethyl-[1,2,5]oxadisilolan-3-one	432.69	377.99	455.43	4.06
10		3-[1-(4-Methanesulfonylphenyl)-4-trifluoromethyl-1*H*-imidazol-2-yl]-pyridine	367.35	275.44	326.64	2.39
10a		3-[1-(4-Methanesulfonylphenyl)-4-trimethylsilanyl-1*H*-imidazol-2-yl]-pyridine	371.53	316.72	368.23	2.81
10b		3-[2-(4-Methanesulfonylphenyl)-4-trifluoromethyl-2*H*-[1,3,2]diazasilol-2-yl]-pyridine	383.42	277.57	329.65	2.69
11		1-(4-Methanesulfonylphenyl)-2-phenyl-4-trifluoromethyl-1*H*-imidazole	366.36	279.89	332.41	3.25
11a		1-(4-Methanesulfonylphenyl)-2-phenyl-4-trimethylsilanyl-1*H*-imidazole	370.54	320.98	373.05	3.82
11b		1-(4-Methanesulfonylphenyl)-2-phenyl-4-trifluoromethyl-2*H*-[1,3,2]diazasilole	382.43	281.49	333.96	3.83

most cases. The larger 15-20% increases in the trimethylsilanyl (**1a**, **2a**, **4a**, **10a** and **11a**) and the dimethylsilole compounds (**1d**, **2d**, **3a-c**, **4d** and **5a**) were the result of further methyl group additions. The calculated Log P (octanol/water) was also increased in most silicon derivatives (Table **1**), reflecting their increased lipophilicity, and hence the possible improvements in their tissue distribution [16].

With an aim at assessing the effects of C-Si replacements in the COX inhibitors on enzyme activity, the structures of the model and sila-substituted compounds were optimized for geometry and then docked with energy minimization in the respective binding sites of the two murine enzyme isoforms. As a control, the ligands originally present in the X-ray crystal structures used for the procedure (respectively Sc-558 (**1**) in COX-2 and flurbiprofen in COX-1) were reconstructed in Brookhaven protein data bank (pdb) format and docked in their respective emptied binding sites. The results generated docked structures with root mean square deviations (RMSD) between the two conformations of 0.05 Å for COX-2/Sc-558 and 0.09 Å for COX-1/flurbiprofen complexes, respectively. These results validate the parameter set used for docking as they indicate its appropriateness to reproduce the original X-ray structures [38]. The minimal energies of binding (E_{bind}) calculated from the docking procedures with each of the model compounds (**1** – **11**, Figs. (**1**)-(**3**)) were directly correlated to their respective experimental inhibitory activities found in the literature (expressed as $pIC_{50} = -\log IC_{50}$), towards both recombinant enzyme isoforms [8, 9, 10, 12, 14, 20, 21, 22, 23, 39, 40, 41]. Such a linear relationship between pIC_{50} and binding energy was consistent with the results reported in another recent *in silico* study with COX-2 inhibitors [41]. The relationships observed in the present study (n = 11) were respectively pIC_{50} (COX-2) = 0.582 – 0.098 E_{bind} (Kcal/mol) and pIC_{50} (COX-1) = – 0.290 – 0.133 E_{bind} (Kcal/mol), with squared correlation coefficients (r^2) of 0.66 for COX-2 and 0.75 for COX-1, respectively. The relatively good accuracy of these correlations further allowed to predict the pIC_{50} of the sila-substituted compounds for both COX isoforms. The selectivity of these inhibitors towards COX-2 is another important parameter, usually estimated by the ratio of COX-1 IC_{50} over COX-2 IC_{50}. With the predicted pIC_{50} data for both COX isoforms in hand, the selectivity of each compound for COX-2 could consequently be predicted. This parameter was expressed as the selectivity index, i.e. the log of the IC_{50} ratio. A cross-validation of the predicted versus the experimental selectivity index obtained from the literature for the 11 model compounds, provided a squared correlation coefficient q^2 of 0.64 and a standard error of prediction of 0.53, validating the accuracy of our predictions to ± 15%. These results are summarized in Table **2**.

Table 2. Results Obtained from Docking the Compounds to COX-2 and COX-1 Binding Sites Using Respectively COX-2/Sc-558 and COX-1/Flurbiprofen as Templates. Comparison of Predicted Versus Experimental Activities of the Respective Compounds Toward Both Isoforms and of Their Selectivity for COX-2

#	Predicted E_{bind} (Kcal/mol) for COX-2	Experimental Activity: pIC_{50}, $-\log IC_{50}$ (COX-2)	Predicted Activity: pIC_{50}, $-\log IC_{50}$ (COX-2)	Predicted E_{bind} (Kcal/mol) for COX-1	Experimental Activity: pIC_{50}, $-\log IC_{50}$ (COX-1)	Predicted Activity: pIC_{50}, $-\log IC_{50}$ (COX-1)	Experimental selectivity index, log pIC_{50} (COX-2) – log pIC_{50} (COX-1)	Predicted selectivity index, log pIC_{50} (COX-2) – log pIC_{50} (COX-1)
1	–73.39	8.05	7.83	–38.86	4.78	4.90	3.28	2.93
1a	–75.97		8.08	–25.12		3.06		5.02
1b	–63.82		6.88	–27.01		3.32		3.56
1c	–81.47		8.63	–25.03		3.05		5.58
1d	–65.22		7.02	–28.47		3.51		3.51
2	–71.75	7.40	7.66	–35.27	4.64	4.42	2.60	3.24
2a	–72.48		7.74	–22.83		2.76		4.98
2b	–66.92		7.19	–22.31		2.69		4.50
2c	–80.27		8.51	–22.06		2.65		5.86
2d	–68.47		7.34	–31.11		3.86		3.47
3	–72.94	7.58	7.78	–30.03	3.00	3.72	4.58	4.06
3a	–67.23		7.22	–12.34		1.35		5.87
3b	–69.91		6.79	–14.34		1.62		5.17
3c	–59.92		6.50	–15.75		1.81		4.69

(Table 2. Contd.)

#	Predicted E_{bind} (Kcal/mol) for COX-2	Experimental Activity: pIC_{50}, $-logIC_{50}$ (COX-2)	Predicted Activity: pIC_{50}, $-log\ IC_{50}$ (COX-2)	Predicted E_{bind} (Kcal/mol) for COX-1	Experimental Activity: pIC_{50}, $-logIC_{50}$ (COX-1)	Predicted Activity: pIC_{50}, $-log\ IC_{50}$ (COX-1)	Experimental selectivity index, log pIC_{50} (COX-2) – log pIC_{50} (COX-1)	Predicted selectivity index, log pIC_{50} (COX-2) – log pIC_{50} (COX-1)
3d	–64.51		6.95	–14.56		1.65		5.29
3e	–66.68		7.17	–13.84		1.56		5.61
4	–68.88	7.40	7.38	–21.51	2.96	2.58	4.45	4.80
4a	–71.55		7.65	–19.35		2.29		5.36
4b	–73.11		7.80	–21.72		2.61		5.19
4c	–63.12		6.81	–19.76		2.35		4.46
4d	–75.05		7.99	–25.89		3.17		4.82
5	–72.51	7.52	7.74	–35.11	4.45	4.42	3.07	3.32
5a	–67.04		7.20	–28.62		3.54		3.66
5b	–69.50		7.44	–14.79		1.68		5.76
5c	–72.08		7.70	–33.06		4.13		3.57
6	–71.94	7.15	7.69	–38.48	4.85	4.85	2.30	2.84
6a	–73.35		7.82	–36.81		4.63		3.19
6b	–79.72		8.45	–49.69		6.35		2.10
7	–64.50	7.00	6.95	–30.08	3.54	3.73	3.46	3.22
7a	–65.25		7.02	–18.24		2.14		4.88
7b	–61.36		6.64	–46.74		5.95		0.69
8	–72.96	8.49	7.79	–26.85	3.40	3.30	5.09	4.49
8a	–74.37		7.93	–14.62		1.66		6.27
8b	–50.95		5.61	–29.97		3.71		1.90
9	–76.40	8.30	8.13	–32.23	4.90	4.02	3.40	4.11
9a	–73.63		7.85	–22.19		2.67		5.18
9b	–63.40		6.84	–32.41		4.04		2.80
9c	–72.63		7.75	–28.47		3.51		4.24
10	–62.19	6.77	6.72	–26.35	3.07	3.23	3.70	3.49
10a	–70.50		7.54	–15.23		1.74		5.80
10b	–60.71		6.58	–27.25		3.35		3.23
11	–62.33	6.88	6.74	–28.42	3.10	3.51	3.78	3.23
11a	–65.94		7.09	–15.12		1.73		5.36
11b	–56.15		6.12	–20.16		2.40		3.72

In most cases, the sila-substitution did not significantly improve the predicted activity for COX-2, except in three instances, where the predicted pIC_{50} was increased by close to one log unit versus the corresponding model compound, namely the diaryldiazasiloles **1c** and **2c**, and the diarylazasiline **6b**. In contrast, the predicted activity for COX-1 was significantly decreased for most of the sila-substituted compounds versus their respective model compounds, except in three cases, namely compounds **6b**, **7b** and **8b**, where the predicted activity for COX-1 was significantly increased. These results are likely to emphasize the importance of the position on cycle C, where rings A and

B are simultaneously attached to the silicon atom. Indeed, the corresponding sila-substituted compounds **6a**, **7a** and **8a**, in which the attachment position of both rings on cycle C is shifted from the original ring B substitution position to that of ring A (see Fig. (**2**)), see instead their predicted activity for COX-1 decreased. Noteworthy also is the significant decrease in predicted activity towards COX-1 observed for many sila-substituted compounds characterized by a poorly conjugated cycle C (e.g. **3a-e**, **5b**, **8a**), although their predicted activity towards COX-2 remains as high as in their respective model compound. This suggests that the change in cycle C conformation induced by the introduction of a silicon atom might be less critical for maintaining COX-2 rather than COX-1 inhibitory activity.

Because the relative changes in activity towards both COX isoforms govern the selectivity for COX-2, it was also interesting to evaluate the possible impact on enzyme activity of the docked compounds geometry within the respective binding sites of COX-1 and COX-2. Amino acid sequences of COX-1 and COX-2 share 67% identity and the overall structures are highly conserved [8]. The COX active sites in the two isoforms are similar with a sequence identity of 87% and strict conservation [42]. Both isoforms contain a primary binding pocket with an accessory secondary pocket gated by Tyr355 and Val523 in COX-2, the latter being replaced by Ile523 in COX-1. The bulkier side chain of Ile523 in COX-1 restricts access of inhibitors to the secondary pocket, which the smaller side chain of Val523 allows in COX-2 [42]. This results in an enlargement of the binding site by 25%, with an available volume increasing from 316 A^3 in COX-1, to 394 A^3 in COX-2 [43, 44]. COX-2 selectivity is considered to be a consequence of preferential interactions of the inhibitor structure with two non-conserved residues within the accessory binding pocket of COX-2, namely Arg513 and Val523 [17]. In COX-1, these interactions occur with His513 and Ile523 and are much weaker [38]. However, other residues within the primary binding pocket have also been identified as critical for COX-2 selectivity. For instance, too strong a charge interaction of the C cycle substituent with Arg120 decreases the association rate of COX-2 inhibitors [45]. In contrast, the same C cycle substituent interacts preferentially with the hydroxyl group of Ser530 side chain of COX-1, which forces the ligand to adopt an alternative position in the primary binding pocket, the B ring being pushed into the hydrophobic hole at its top, made by Tyr385 and Trp387 [17]. Increased activity for COX-1 is thus dependent on the strength of interaction of the B ring with Tyr385, on the decrease in the interaction of the C cycle substituent with Arg120, and on its resulting improved interaction with Ser530 [17, 44]. In selective COX-2 inhibitors, the loss of favorable B ring interaction with Tyr385 allows for the A ring to penetrate deeper into the accessory secondary binding pocket, which induces the sulfonamide or methanesulfonyl oxygens to establish H-bonds with Arg513 and His90, and the amido or methyl groups to interact with the hydrophobic chain made by Phe518, Leu352 and Ser353 [14, 38, 39, 41, 44, 46]. This is the result of strong van der Waals contacts of the C cycle substituent with Leu531 and Leu117 in the primary binding pocket [39, 41], although an H-bond remains possible with the hydroxyl group of Ser530, thanks to its specific rotation to a down-conformation in the COX-2 structure [44].

When examining the docked structures for interactions with the selected residues mentioned above, the advantages brought by the sila-substitution were found to result from changes in the distance of the inhibitor structure from these residues in the respective binding sites, that were completely in line with the previous observations. Increased activity towards COX-2 was mainly governed by the depth with which ring A penetrates into the secondary binding pocket of the isoform with increased H-bonding of the sulfonyl oxygens, particularly with His90. In contrast, increased activity towards COX-1 was primarily the consequence of an increased interaction of ring B with Tyr385, due to the strength of contact between the cycle C substituent and Ser530. The changes in activity of the sila-substituted compounds towards both enzyme isoforms and the resulting changes in selectivity for COX-2 as compared to the respective model compounds, are the consequence of the changes in bond lengths and bond angles due to the carbon-silicon replacement. This is best illustrated in Figs. (**4**) to (**7**) with the docked structures of two extreme examples (see Table **2**) presented by the respective compound pairs **1**/**1c** and **6**/**6b**. On one hand, compound **1c** shows an increased predicted activity for COX-2 and a decreased predicted activity for COX-1, resulting in a predicted selectivity index for COX-2 that jumps from 2.93 to 5.58, when compared to the model Sc-558 (**1**). On the other hand, the similar increase in predicted activity towards COX-2 of compound **6b** is matched by a strong increase of the predicted activity for COX-1, which results in a predicted selectivity index that drops slightly from 2.84 to 2.10, when compared to the model compound Etoricoxib (**6**).

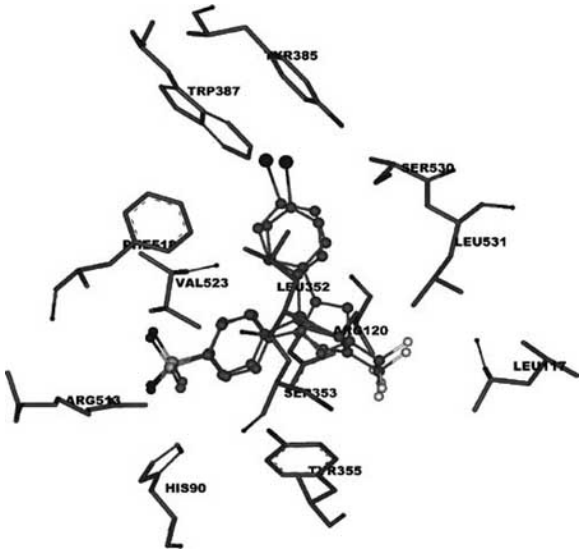

Fig. (4). Superimposition of the docked structures **1** and **1c** (ball and sticks) within the COX-2 binding site (residues in sticks). Hydrogens have been removed for clarity. The increased predicted activity of **1c** (see Table **2**) can be ascribed to a deeper penetration of the A ring within the accesssory secondary pocket resulting from the length of the Si-C bond with ring A, whilst the Si-C cycle rotation does not modify significantly the interactions within the primary pocket.

The minimized structures of both sila-substituted **1c** and **6b** within the active site of COX-2 (Figs (**4**) and (**5**)), fit with those of their respective model compounds **1** and **6**. Rings A and B are in similar planes, whilst the Si-C substitution imparts a rotation to the cycle C plane by approximately 90°. But because the rotational angle leaves the respective CF_3 and Cl substituents close to their original orientation, this does not significantly alter the distances from, and hence the interactions with Leu117 and Leu531 within the primary pocket of the binding site. For instance, the distance of the respective CF_3 and Cl substituents from the $-CH(CH_3)_2$ side chain group of Leu117, change from 8.21 (**1**) to 8.25 Å (**1c**) and from 8.53 (**6**) to 8.88 Å (**6b**), respectively. The rotational angle of cycle C in the sila-substituted compounds however removes the same substituents from Arg120. The respective distances from the closer NH_2 of Arg120 change from 3.12 (**1**) to 3.37 Å (**1c**) and from 3.81 (**6**) to 4.24 Å (**6b**). The increased length of the Si-C bond with ring A also results in its deeper penetration within the accessory secondary pocket. In each case, the distance between the sulfonyl *S* atom and the side chain of Val523 is increased by over 0.1 Å when compared to the respective model compounds, which on a futher slight orientation change of ring A, results in closer H-bonds of the sulfonyl oxygens with the NH_2 of Arg513 and His90 by 0.2 and 0.3 Å in average, respectively. Such increases in H-bonding capacity of the sulfonyl oxygens in the secondary binding pocket, along with the slight increase in distance of the C cycle substituent from Arg120 in the primary pocket, are sufficient to explain the predicted increases in pIC_{50} by one log unit (see Table **2**) [14, 43, 45].

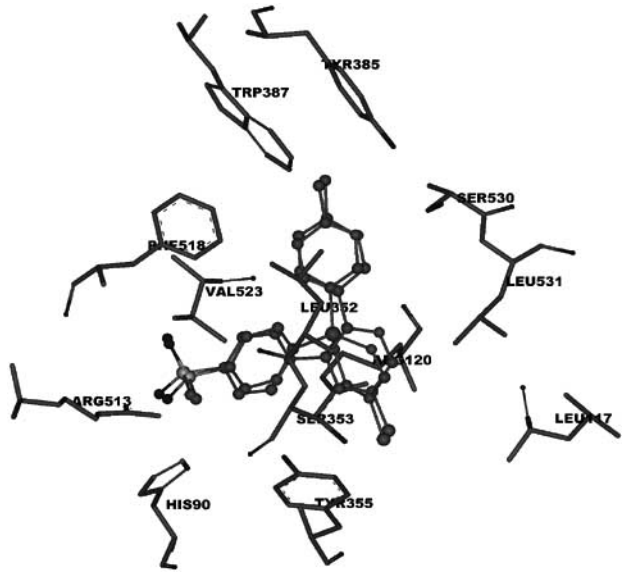

Fig. (5). Superimposition of the docked structures **6** and **6b** (ball and sticks) within the COX-2 binding site (residues in sticks). Hydrogens have been removed for clarity. The increased predicted activity of **6b** (see Table **2**) can be ascribed to a deeper penetration of the A ring within the accesssory secondary pocket resulting from the length of the Si-C bond with ring A, whilst the Si-C cycle rotation does not modify significantly the interactions within the primary pocket.

Within the COX-1 binding site (Figs (**6**) and (**7**)), the minimized structure geometry of the same sila-substituted compounds differ more significantly from those of their respective model compounds, which explains their divergent behaviors in predicted inhibitory activity towards the enzyme. In the case of **1c** (Fig. (**6**)), the rotational angle of cycle C imparted by the sila-substitution, removes the CF_3 substituent from the hydroxyl group of Ser530 by 1.34 Å, which consequently removes ring B from Tyr385 by approximately the same distance and brings the sulfonyl substituent of ring A closer to His513. The C cycle rotation also brings the CF_3 substituent in better contact with one NH_2 of Arg120 by 1.07 Å. This explains the decrease in predicted pIC_{50} of **1c** for COX-1 by close to two log units, when compared to **1** (Table **2**) [17, 38, 44]. In contrast, the rotational angle of cycle C imparted by the sila-substitution in **6b** (Fig. (**7**)), brings the Cl substituent closer to Ser530 by 2.57 Å when compared to the model compound **6**, which not only results in a deeper penetration of ring B in the hydrophobic pocket made by Tyr385-Trp387 by 0.53 Å, but also removes the sulfonyl group from His90 and Arg513 by 0.25 Å in average, and removes the C cycle Cl substituent from Arg120 by 0.71 Å. This difference in orientation within the COX-1 binding site explains the increased predicted pIC_{50} of **6b** by 1.5 log unit when compared to the parent compound **6** (Table **2**) [17, 38, 44]. Thus, despite a similar geometry of insertion between the respective pairs **1**-**1c** and **6**-**6b** within the COX-2 binding site, with improvements in critical contacts explaining the increase in predicted pIC_{50} for the sila-substituted compounds, the different orientations between the same pairs within the COX-1 binding site and the resulting opposite differences in predicted inhibitory activity, explain the increase in predicted selectivity index for COX-2 of the former pair of compounds and the relative selectivity index stability of the latter.

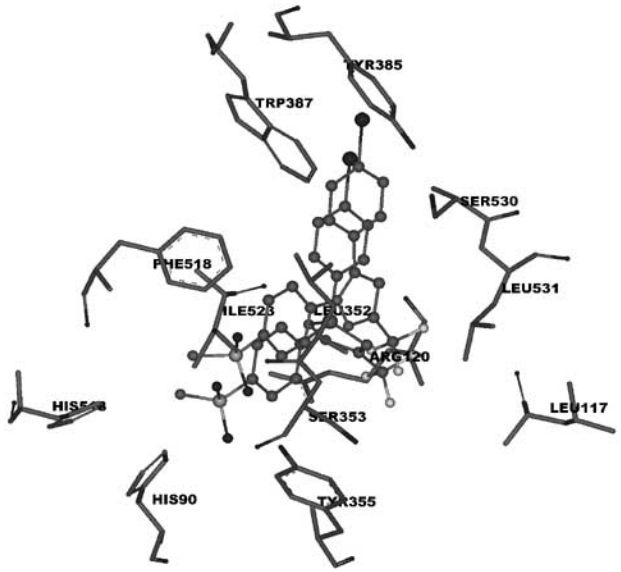

Fig. (6). Superimposition of the docked structures **1** and **1c** (ball and sticks) within the COX-1 binding site (residues in sticks). Hydrogens have been removed for clarity. The decreased predicted activity of **1c** (see Table **2**) can be ascribed to a loss of contact of the B ring with Tyr385, resulting from a decreased interaction of the C cycle CF_3 substituent with Ser530 due to the Si-C cycle rotation.

The preliminary results obtained during the present study by a comparative computational docking evaluation of sila-substituted COX-2 inhibitors are likely to indicate that suitable sila-substitutions could allow to modulate the selectivity of NSAIDs for COX isozymes.

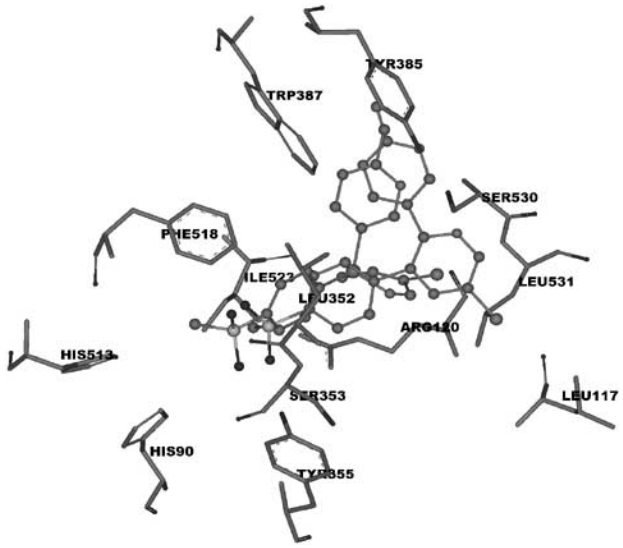

Fig. (7). Superimposition of the docked structures **6** and **6b** (ball and sticks) within the COX-1 binding site (residues in sticks). Hydrogens have been removed for clarity. The increased predicted activity of **6b** (see Table **2**) can be ascribed to an increased contact of the B ring with Tyr385, resulting from an increased interaction of the C cycle Cl substituent with Ser530 due to the Si-C cycle rotation.

METHODS

The ligand molecules were constructed in pdb format using the DS viewerPro program from Accelrys Inc and were energy minimized with a convergence of 0.01 Kcal/mol using the Alchemy 2000 program from Tripos Inc. The SciLogP module of the Alchemy 2000 program was then used to calculate the molecular weight (M.W.), volume, surface and the octanol/water partition coefficient (LogP) of each compound. The respective X-ray crystal structures of murine COX-2 complexed with Sc-558 (entry code 6COX) [8] and murine COX-1 complexed with flurbiprofen (entry code 1CQE) [47] were obtained from the pdb. The structures were stripped of ligand and water molecules. The docking experiments were performed by spherical polar Fourier correlations using the Hex 4.2 program (http://www. biochem.abdn.ac.uk) [48]. The enzyme structure stripped of inhibitor was used as the receptor and hydrogens were added. The original structure containing the inhibitor was used as complex template. The ligand was fit on the template and docking within the receptor was performed with full rotation allowed by 1280 steps of 5 degree (deg.) each, and a twist angle search of +/- 7.5 deg. by steps of 1.4 deg. from the starting orientation, within a distance range of 5 Å by steps of 0.1 Å. Molecular mechanics energy minimization was applied and used to calculate the total binding energy (E_{bind}) for each docking solution, from which the one with the lowest E_{bind} was selected. The distances between atoms of the energy minimized docked ligand structures and atoms of residues within the respective COX binding sites were evaluated using the DS Viewer Pro program. The cross-validated squared coefficient of correlation q^2 within the model compounds group , between experimental (exp.) and predicted (pred.) selectivity index (SI) for COX-2, was calculated using the following formula:

$$q^2 = 1 - \frac{\sum (SI_{\text{exp.}} - SI_{pred.})^2}{\sum (SI_{\text{exp.}} - SI_{mean})^2}$$

with the standard error of prediction ($SE_{pred.}$) calculated according to the formula:

$$SE_{pred.} = \sqrt{\frac{\sum (SI_{pred.} - SI_{\text{exp.}})^2}{n-2}}$$

where n is the number of observations.

REFERENCES

[1] Dubois, R.N.; Abramson, S.B.; Crofford, L.; Gupta, R.A.; Simon, L.S.; van de Pute, L.B.;Lipsky, P.E. *FASEB J.*, **1998**, *12*, 1063.
[2] Vane, J.R. *Nature New Biol.*, **1971**, *231*, 232.
[3] Smith, W.L.; Garavito, R.M.; DeWitt, D.L. *J. Biol. Chem.*, **1996**, *271*, 33157.
[4] Englebienne, P. *Drug Design Rev. – Online*, **2004**, *1*, 53.
[5] Marnett, L.J.; Kagutkar, A.S. *Curr. Opin. Chem. Biol.*, **1998**, *2*, 482.
[6] Gately, S.; Li, W.W. *Semin. Oncol.*, **2004**, *31* (Suppl. 7), 2.
[7] Fabiola, G.F.; Pattabhi, V.; Nagarajan, K. *Bioorg. Med. Chem.*, **1998**, *6*, 2337.
[8] Kurumbail, R.G.; Stevens, A.M.; Gierse, J.K.; McDonald, J.J.; Stegeman, R.A.; Pak, J.Y.; Gildehaus, D.; Miyashiro, J.M.; Penning, T.D.; Seibert, K.; Isakson, P.C.; Stallings, W.C. *Nature*, **1996**, *384*, 644.
[9] Prasit, P.; Riendeau,D. *Annu. Rep. Med. Chem.*, **1997**, *32*, 211.
[10] Talley, J.J.; Brown, D.L.; Carter, J.S.; Graneto, M.J.; Koboldt, C.M.; Masferrer, J.L.; Perkins, W.E.; Rogers, R.S.; Shaffer, A.F.; Zhang, Y.Y.; Zweifel, B.S.; Seibert, K. *J. Med. Chem.*, **2000**, *43*, 775.
[11] Prasit, P.; Wang, Z.; Brideau, C.; Chan, C.C.; Charleson, S.; Cromlish, W.; Ethier, D.; Evans, J.F.; Ford-Hutchinson, A.W.; Gauthier, J.Y.; Gordon, R.; Guay, J.; Gresser, M.; Kargman, S.; Kennedy, B.; Leblanc, Y.; Léger, S.; Mancini, J.; O'Neill, G.P.; Ouellet, M.; Percival, M.D.; Perrier, H.; Riendeau, D.; Rodger, I.; Tagari, P.; Thérien, M.; Vickers, P.; Wong, E.; Xu, L.J.; Young, R.N.; Zamboni, R. *Bioorg. Med. Chem. Lett.*, **1999**, *9*, 1773.
[12] Friesen, R.W.; Brideau, C.; Chan, C.C.; Charleson, S.; Deschênes, D.; Dubé, D.; Ethier, D.; Fortin, R.; Gauthier, J.Y.; Girard, Y.; Gordon, R.; Greig, G.M.; Riendeau, D.; Savoie, C.; Wang, Z.; Wong, E.; Visco, D.; Xu, L.J.; Young, R.N. *Bioorg. Med. Chem. Lett.*, **1998**, *8*, 2777.
[13] Habeeb, A.G.; Rao, P.N.P.; Knaus, E.E. *J. Med. Chem.*, **2001**, *44*, 3039.
[14] Uddin, M.J.; Rao, P.N.P.; Knaus, E.E. *Bioorg. Med. Chem. Lett.*, **2003**, *11*, 5273.
[15] Singh, S.K.; Vobbalareddy, S.; Shivaramakrishna, S.; Krishnamraju, A.; Rajjak, S.A.; Casturi, S.R.; Akhila, V.; Rao, Y.K. *Bioorg. Med. Chem. Lett.*, **2004**, *14*, 1683.
[16] Showell, G.A.; Mills, J.S. *Drug Discovery Today*, **2003**, *8*, 551.
[17] Filizola, M.; Perez, J.J.; Palomer, A.; Mauleon, D. *J. Mol. Graphics Model.*, **1997**, *15*, 290.
[18] Campbell, S.J.; Gold, N.D.; Jackson, R.M.; Westhead, D.R. *Curr. Opin. Struct. Biol.*, **2003**, *13*, 389.
[19] Alvarez, J.C. *Curr. Opin. Chem. Biol.*, **2004**, *8*, 1.
[20] Li, J.J.; Anderson, G.D.; Burton, E.G.; Cogburn, J.N.; Collins, J.T.; Garland, D.J.; Gregory, S.A.; Huang, H.C.; Isakson, P.C.; Koboldt, C.M.; Logusch, E.W.; Norton, M.B.; Perkins, W.E.; Reinhard, E.J.;

Seibert, K.; Veenhuizen, A.W.; Zhang, Y.; Reitz, D.B. *J. Med. Chem.*, **1995**, *38*, 4570.
[21] Shin, S.S.; Byun, Y.; Lim, K.M.; Choi, J.K.; Lee, K.W.; Moh, J.H.; Kim, J.K.; Jeong, Y.S.; Kim, J.Y.; Choi, Y.H.; Koh, H.J.; Park, Y.H.; Oh, Y.I.; Noh, M.S.; Chung, S. *J. Med. Chem.*, **2004**, *47*, 792.
[22] Rao, P.N.P.; Amini, M.; Li, H.; Habeeb, A.G.; Knaus, E.E. *J. Med. Chem.*, **2003**, *46*, 4872.
[23] Khanna, I.K.; Yu, Y.; Huff, R.M.; Weier, R.M.; Xu, X.; Koszyk, F.J.; Collins, P.W.; Cogburn, J.N., Isakson, P.C.; Koboldt, C.M.; Masferrer, J.L.; Perkins, W.E.; Seibert, K.; Veenhuizen, A.W.; Yuan, J.; Yang, D.C.; Zhang, Y.Y. *J. Med. Chem.*, **2000**, *43*, 3168.
[24] Ezbiansky, K.; Djurovich, P.I.; LaForest, M.; Sinning, D.J.; Zayes, R.; Berry, D.H. *Organometallics*, **1998**, *17*, 1455.
[25] Kakiuchi, F.; Matsumoto, M.; Tsuchiya, K.; Igi, K.; Hayamizu, T.; Chatani, N.; Murai, S. *J. Organometal. Chem.*, **2003**, *686*, 134.
[26] Ishikawa, M.; Okazaki, S.; Naka, A.; Sakamoto, H. *Organometallics*, **1992**, *11*, 4135.
[27] Yamaguchi, S.; Tamao, K. *J. Chem. Soc., Dalton Trans.*, **1998**, 3693.
[28] Tang, B.Z.; Zhan, X.; Yu, G.; Lee, P.P.S.; Liu, Y.; Zhu, D. *J. Mater. Chem.*, **2001**, *11*, 2974.
[29] Cai, Y.; Roberts, B.P. *J. Chem. Soc., Perkin Trans. 1*, **1998**, 467.
[30] Losehand, U.; Mitzel, N. W. *J. Chem. Soc., Dalton Trans.*, **2000**, 1049.
[31] Bowman, W.R.; Cloonan, M.O.; Krintel, S.L. *J. Chem. Soc., Perkin Trans. 1*, **2001**, 2885.
[32] Sakai, N.; Fukushima, T.; Okada, O.; Ohashi, S.; Minakata, S.; Komatsu, M. *J. Organometal. Chem.*, **2003**, *686*, 368.
[33] Heinonen, P.; Sipilä, H.; Neuvonen, K.; Lönnberg, H.; Cockcroft, V.B.; Wurster, S.; Virtanen, R.; Savola, M.K.T.; Salonen, J.S.; Savola, J.M. *Eur. J. Med. Chem.*, **1996**, *31*, 725.
[34] Felder, C.C.; Bymaster, F.P.; Ward, J.; DeLapp, N. *J. Med. Chem.*, **2000**, *43*, 4333.
[35] Tacke, R.; Handmann, V.I.; Kreutzmann, K.; Keim, C.; Mutschler, E.; Lambrecht, G. *Organometallics*, **2002**, *21*, 3727.
[36] Tacke, R.; Handmann, V.I.; Bertermann, R.; Burschka, C.; Penka, M.; Seyfried, C. *Organometallics*, **2003**, *22*, 916.
[37] Heinrich, T.; Burschka, C.; Warneck, J.; Tacke, R. *Organometallics*, **2004**, *23*, 361.
[38] Liu, H.; Huang, X.; Shen, J.; Luo, X.; Li, M.; Xiong, B.; Chen, G.; Shen, J.; Yang, Y.; Jiang, H.; Chen, K. *J. Med. Chem.*, **2002**, *45*, 4816.
[39] Desiraju, G.R.; Gopalakrishnan, B.; Jetti, R.K.R.; Nagaraju, A.; Raveendra, D.; Sarma, J.A.R.P.; Sobhia, M.E.; Thilagavathi, R. *J. Med. Chem.*, **2002**, *45*, 4847.
[40] Rao, P.N.; Amini, M.; Li, H.; Habeeb, A.G.; Knaus, E.E. *Bioorg. Med. Chem. Lett.*, **2003**, *13*, 2205.
[41] Kim, H.J.; Chae, C.H.; Yi, K.Y.; Park, K.L.; Yoo, S. *Bioorg. Med. Chem.*, **2004**, *12*, 1629.
[42] Fabiola, G.F.; Pattabhi, V.; Nagarajan, K. *Bioorg. Med. Chem.*, **1998**, *6*, 2337.
[43] Pal, M.; Madan, M.; Padakanti, S.; Pattabiraman, V.R.; Kalleda, S.; Vanguri, A.; Mullangi, R.; Mamidi, N.V.S.R.; Casturi, S.R.; Malde, A.; Gopalakrishnan, B.; Yeleswarapu, K.R. *J. Med. Chem.*, **2003**, *46*, 3975.
[44] Soliva, R.; Almansa, C.; Kalko, S.G., Luque, F.J.; Orozco, M. *J. Med. Chem.*, **2003**, *46*, 1372.
[45] Hood, W.F.; Gierse, J.K.; Isakson, P.C.; Kiefer, J.R.; Kurumbail, R.G.; Seibert, K.; Monahan, J.B. *Mol. Pharmacol.*, **2003**, *63*, 870.
[46] Palomer, A.; Cabré, F.; Pascual, J.; Campos, J.; Trujillo, M.A.; Entrena, A.; Gallo, M.A.; Garcia, L.; Mauleon, D.; Espinosa, A. *J. Med. Chem.*, **2002**, *45*, 1402.
[47] Picot, D.; Loll, P.J.; Garavito, R.M. *Nature*, **1994**, *367*, 243.
[48] Ritchie, D.W.; Kemp, G.J.L. *J. Comp. Chem.*, **1999**, *20*, 383.

Received: 29 July, 2004 Accepted: 17 January, 2005